167. Synthesis of $[Ir_3Rh(CO)_{12}]$ and Fluxional Behaviour of Some of Its Substituted Derivatives

by **Giacomo Bondietti**[1]), **Gábor Laurenczy, Renzo Ros**[2]), and **Raymond Roulet***

Institut de Chimie Minérale et Analytique, Université de Lausanne, BCH, CH-1015 Lausanne

(7.VI.1994)

The redox condensation of $[Ir(CO)_4]^-$, $[Ir(cod)(THF)_2]^+$, and $[Rh(cod)(THF)_2]^+$ (cod = cycloocta-1,5-diene) followed by saturation with CO (1 atm) in THF afforded the first synthetic route to pure $[Ir_3Rh(CO)_{12}]$ (**1**). Substitution of CO by monodentate ligands gave $[Ir_3Rh(CO)_8(\mu_2\text{-}CO)_3L]$ (L = Br^-, **2**; I^-, **3**; bicyclo[2.2.1]hept-2-ene, **4**; PPh_3, **5**). Clusters **2**–**5** have C_s symmetry with the ligand L bound to the basal Rh-atom in axial position. They are fluxional in solution at the NMR time scale due to two CO scrambling processes: the merry-go-round of basal CO's and changes of basal face. An additional process takes place in **5** above room temperature: the intramolecular migration of PPh_3 from the Rh- to a basal Ir-atom. Substitution of CO by polydentate ligands gave $[Ir_3Rh(CO)_{7-x}(\mu_2\text{-}CO)_3(\eta^4\text{-}L)_x]$ (L = bicyclo[2.2.1]hepta-2,5-diene (= norbornadiene; nbd), $x = 1$, **6**; L = nbd, $x = 2$, **13**; L = cod, $x = 1$, **7**; L = cod $x = 2$, **15**), $[Ir_3Rh(CO)_7(\mu_2\text{-}CO)_3(\eta^2\text{-diars})]$ (diars = 1,2-phenylenebis-(dimethylarsine); **8**), $[Ir_3Rh(CO)_7(\mu_2\text{-}CO)_3(\eta^4\text{-}L)]$ (L = methylenebis(diphenylphosphine), bonded to 2 basal Ir-atom (**9a**) or one Ir- and one Rh-atom (**9b**)), $[Ir_3Rh(CO)_6(\mu_2\text{-}CO)_3(\eta^4\text{-nbd})PPh_3]$ (**12**), and $[Ir_3Rh(CO)_6(\mu_2\text{-}CO)_3(\mu_3\text{-}L)]$ (L = 1,3,5-trithiane, **10**; L = $CH(PPh_2)_3$, **11**). Complexes **6**–**8**, **9a**, **10**, and **11** have C_s symmetry, the others C_1 symmetry. They are fluxional in solution due to CO scrambling processes involving 1, 3, or 4 metal centres as deduced from 2D-EXSY spectra. Comparison of the activation energies of these processes with those of the isostructural Ir_4 and Ir_2Rh_2 compounds showed that substitution of Ir by Rh in the basal face of an Ir_4 compound slows the processes involving 3 or 4 metal centres (merry-go-round and change of basal face), but increases the rate of carbonyl rotation about an Ir-atom.

Introduction. – The tetrahedral carbonyl cluster compounds of mixed d^9 metals known to date are $[Co_xRh_{4-x}(CO)_{12}]$ ($x = 2$, 3) [1] [2], $[Co_2Ir_2(CO)_{12}]$ [1] [3], and $[Ir_xRh_{4-x}(CO)_{12}]$ ($x = 1$, 2) [1] [4]. $[CoRh_3(CO)_{12}]$ and $[CoIr_3(CO)_{12}]$ are thermally unstable [1] [5], and $[Ir_3Rh(CO)_{12}]$ could not be obtained by standard redox condensation of two monomeric complexes of Ir^{-I} and Rh^{III} or by the reaction of $[Rh(CO)_4]^-$ with $[Ir_4(CO)_{12}]$.

We report here a redox cocondensation method giving pure $[Ir_3Rh(CO)_{12}]$ (**1**), the preparation of some of its substituted derivatives, and a NMR study of their fluxional behaviour in solution.

Results and Discussion. – 1. *Synthesis of $[Ir_3Rh(CO)_{12}]$.* The redox condensation of $[Ir(CO)_4]^-$, $[Ir(cod)(THF)_2]^+$, and $[Rh(cod)(THF)_2]^+$ (cod = cycloocta-1,5-diene) in the molar ratios 2:1:1 yielded $[Ir_3Rh(CO)_5(\mu_2\text{-}CO)_3(\eta^4\text{-cod})_2]$. Diene displacement was achieved by stirring the latter compound in THF under CO (1 atm) giving pure $[Ir_3Rh(CO)_{12}]$ (**1**; overall yield 21%). The orange-yellow crystals of **1** were found highly disordered, unlike those of $[Ir_3Rh(CO)_5(\mu_2\text{-}CO)_3(\eta^4\text{-cod})_2]$ whose structure was estab-

[1]) In part from the Ph. D. Thesis of *G. B.*, No. 1135, EPF-Lausanne.

[2]) Permanent address: Instituto di Chimica Industriale dell'Università, Via Marzolo 9, I-35131 Padova.

lished by single-crystal X-ray diffraction [6]. The low solubility of **1** in common organic solvents (< 0.005M) prevented its characterisation by ^{13}C-NMR spectroscopy. The IR spectrum of a dispersion of **1** in nujol shows a strong and broad absorption at 2057 cm^{-1}, indicating a geometry with all CO's terminal in the solid state. Its IR spectrum in CH_2Cl_2 displays two bands below 1900 cm^{-1} due to an isomer with bridging CO's and is similar to those of its monosubstituted derivatives which are fully characterised by ^{13}C-NMR spectroscopy (see below).

2. *Monosubstituted Complexes.* The reaction of **1** with excess $[NEt_4]X$ in THF yielded $[NEt_4]$ $[Ir_3Rh(CO)_{11}X]$ (X = I^-, **2**; Br^-, **3**) on crystallisation from THF/MeOH. These complexes reverted back to **1** in solution under CO (1 atm). The chloro complex is thermally unstable and could not be isolated. The IR spectra of **2** and **3** in THF or CH_2Cl_2 show two absorptions in the region of 1900–1800 cm^{-1} indicating the presence of bridging CO's. The ^{13}C-NMR spectra of samples of **2** and **3** enriched in ^{13}CO (*ca.* 30%) are quite similar (see *Exper. Part*). A *doublet* and a *singlet* with relative intensities 2:1 are observed in the region of bridging CO's and also in the region of radial CO's, but with inverse relative intensities. The C,Rh-coupling constants (32 and 80 Hz, resp.) are quite comparable to those observed in $[Rh_4(CO)_{12}]$ for bridging and radial CO's, respectively [7]. The remaining resonances are 3 *singlets* with relative intensities 1:2:2. The latter two resonances show cross-peaks in a 2D-COSY spectrum and are due to pairs of terminal CO's in pseudo-*trans* positions. Therefore, the ground-state geometry of **2** and **3** is C_s with the halide ligand bonded to the basal Rh-atom in axial position (*Scheme 1*).

Scheme 1

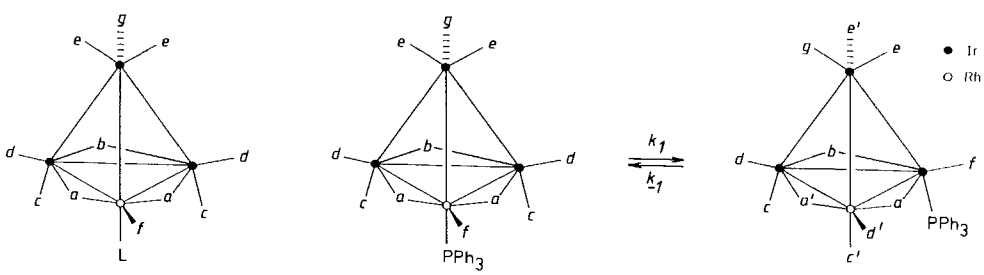

1 L = CO
2 L = I, $[NEt_4]$ salt
3 L = Br, $[NEt_4]$ salt
4 L = norborn-2-ene

5a **5b**

Both complexes are fluxional in solution above *ca.* 200 K. A 2D-EXSY spectrum of **2** in CD_2Cl_2 at 245 K (mixing time: 100 ms; *Fig. 1*) shows two sets of dynamic connectivities. The exchange $f \leftrightarrow a \leftrightarrow d \leftrightarrow b$ corresponds clearly to the merry-go-round of 6 CO's about the basal Ir_2Rh face. The second set also involves 6 CO's (*d*, *c*, and *e*). Since exchanges between basal and apical CO's are observed, the proposed mechanism consists of two successive changes of basal face, the second one being needed to restore the halide ligand in its initial, axial position. In addition, the changes of basal face must be synchronous, *i.e.*, must not pass through an unbridged intermediate, since the edge-bridging CO's *a* and *b* do not participate in the observed exchange. A successful simulation of the variable-temperature ^{13}C-NMR spectra was obtained using the following exchange

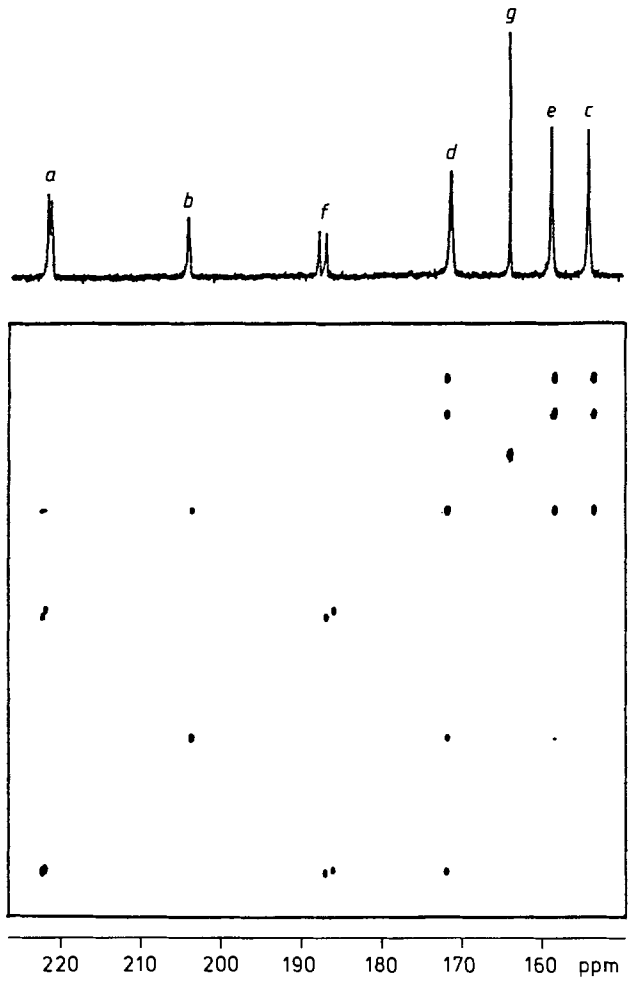

Fig. 1. *2D-EXSY ^{13}C-NMR Spectrum of $[NEt_3][Ir_3Rh(CO)_{11}]$* (**2**) *in CD_2Cl_2 at 245 K*

matrix elements: $(a,a) = (b,b) = (f,f) = -k_1$, $(a,d) = (a,f) = (d,a) = (d,b) = k_1/2$, $(b,d) = (f,a) = k_1$, $(c,c) = (e,e) = -k_2$, $(c,d) = (c,e) = (d,c) = (d,e) = (e,c) = (e,d) = k_2/2$ and $(d,d) = -k_1 \cdot -k_2$, with k_1 = rate constant of the merry-go-round and k_2 = rate constant of the changes of basal face. *Eyring* regressions of $\ln(k/T)$ *vs.* $1/T$ gave the following values of $\Delta G^{\ddagger}$ at 298 K: 51.6 ± 0.3 (**2**) and 51.7 ± 0.6 (**3**) for the merry-go-round, 52.4 ± 0.5 (**2**) and 51.7 ± 0.4 kJ mol^{-1} (**3**) for the changes of basal face. As the $\Delta G^{\ddagger}$'s of the two processes are equal within experimental error, it is possible that there is one common transition state, but we failed to fit all the cross-peak volumes of the 2D-EXSY spectra using one rate constant only. It is, therefore, postulated that in the intermediate of the merry-go-round (**I** in *Scheme 2*), there are two semi-bridging CO's to the electron-rich Rh-X centre. The presence of the semi-bridging CO's prevents the formation of **II** directly from **I**. As previously proposed for $[Ir_4(CO)_{11}L]$ (L = Br^- [8], PEt_3 [9]), both mechanisms involve

concerted bridge formation during the bridge opening, rather than the *Cotton* mechanism of concerted bridge opening followed by bridge closing. The basicity of the halide ligand has no significant influence on the free enthalpy of activation of the CO-scrambling processes, as observed previously for $[Ir_4(CO)_{11}X]^-$ (38.6 ± 0.3 and 36.8 ± 0.3 for X = I^-, 37.0 ± 1.2 [10] and 35.0 ± 0.8 kJ mol^{-1} for X = Br^- [8]). The comparison between the $\Delta G^{\ddagger}$'s of **2** and **3** and those of the related Ir_4 compounds shows that the activation energy of both processes increases by *ca.* 15 kJ mol^{-1} on substituting one Ir- by a Rh-atom. This effect is observed in all derivatives of $[Ir_3Rh(CO)_{12}]$ (see below).

Scheme 2

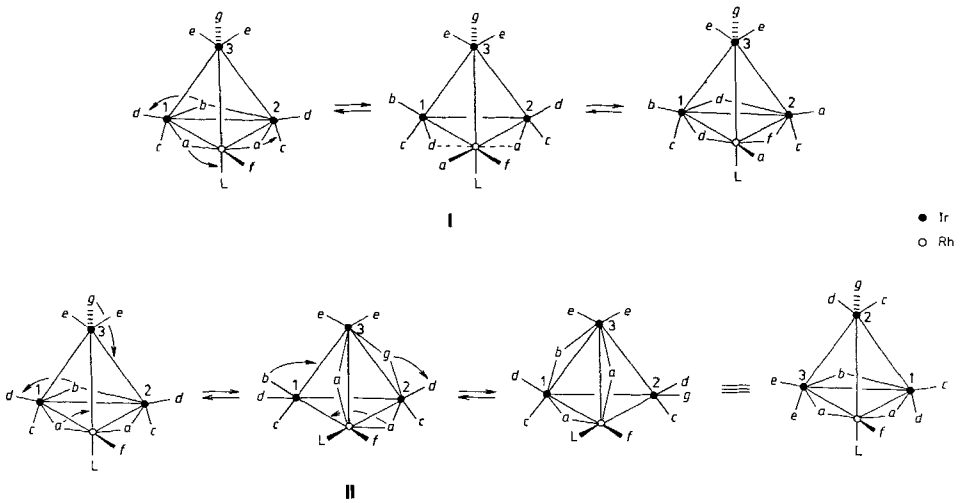

The reaction of **3** with 1 mol-equiv. of norbornene (= bicyclo[2.2.1]hept-2-ene) in the presence of $AgBF_4$ gave $[Ir_3Rh(CO)_8(\mu_2\text{-}CO)_3(\eta^2\text{-norbornene})]$ (**4**) which could not be isolated in the solid state, but whose ^{13}C-NMR spectrum in CD_2Cl_2 at 233 K is quite similar to those of **2** and **3** (see *Exper. Part*). A 2D-EXSY spectrum shows the same dynamic connectivities as for **2** and **3**, and line-shape analysis of the variable-temperature ^{13}C-NMR spectra gave a $\Delta G^{\ddagger}$ (at 298 K) of 53.4 ± 0.8 kJ mol^{-1} for the merry-go-round and of 56.8 ± 0.8 kJ mol^{-1} for the changes of basal face.

The reaction of **2** with 1 mol-equiv. of PPh_3 and of $AgClO_4$ in THF at 263 K followed by chromatography gave $[Ir_3Rh(CO)_{11}PPh_3]$ (**5**; 66%). Its ^{31}P-NMR spectrum in CD_2Cl_2 presents a *doublet* (J(P,Rh) = 122 Hz) and a *singlet* with relative intensities 3:1. Two isomers are present in solution with the PPh_3 ligand either bonded to Rh (**5a**) or to Ir (**5b**; see *Scheme 1*). Isomer **5a** is the kinetically favoured product, since rapid displacement of the labile olefinic ligand in **4** by 1 mol-equiv. of PPh_3 in THF at 263 K gave **5a** and **5b** in the molar ratio 16:1. The two isomers could not be separated using chromatography or fractional crystallisation. However, a pure sample of **5b** was obtained by taking advantage of the faster substitution reaction at a Rh- than at an Ir-atom. A mixture of the two isomers was refluxed in CH_2Cl_2 in the presence of norbornadiene (nbd = bicyclo[2.2.1]hepta-2,5-diene) giving $[Ir_3Rh(CO)_9(\eta^4\text{-nbd})PPh_3]$ with the diolefin

bonded to Rh. The latter cluster was separated from unreacted **5a** by chromatography, then treated with CO (1 atm) to form **5b**. The IR spectrum of **5b** presents two absorptions below 1900 cm^{-1} indicating the presence of bridging CO's. The ^{13}C-NMR spectrum of a sample of **5b** enriched in ^{13}CO (*ca.* 30%) in CD_2Cl_2 at 170 K presents 11 resonances with equal relative intensities (see *Exper. Part*). Three resonances have δ's in the region of bridging CO's. Three others appear in the region of radial CO's, one of these presenting a C,Rh coupling (*d'*) and a second one a geminal C,P coupling (*f*). A 2D-COSY spectrum shows cross-peaks between the radial CO's *d'*, *f*, and *d*. Therefore, the ground-state geometry of **5b** has C_1 symmetry with 3 μ_2-CO's defining the basal Ir_2Rh face and with PPh_3 bonded to a basal Ir-atom in axial position. The ^{13}C-NMR spectrum of the mixture of isomers presents 7 additonal resonances due to **5a** with relative intensities 2:1:1:2:1:2:2 in the order of decreasing δ's. The two resonances with highests δ's are characteristic of bridging CO's. A *doublet* of *doublet* (J(C,Rh) = 78.0, J(C,P) = 6.4 Hz, *f*), and a *singlet* (*d*) with relative intensities 1:2 appear in the region of radial CO's, and a pseudo-*cis* C,C coupling is observed between these two resonances in a 2D-COSY spectrum (see *Exper. Part*). Therefore, the ground-state geometry of **5a** has C_s symmetry with PPh_3 bonded to the basal Rh-atom in axial position (see *Scheme 1*).

The variable-temperature ^{31}P-NMR spectra ($289 < T < 321$ K) of **5** in CD_2Cl_2 (0.06M, *ca.* 90% of **5a** initially) show a decrease of intensity of the *doublet* (**5a**) and a corresponding increase of intensity of the *singlet* (**5b**). Therefore, an isomerisation **5a** $\rightleftharpoons$ **5b** takes place in solution above room temperature. This is the second example to date of a migration of the reputedly inert PPh_3 ligand between two metal centres, quite similar to that observed in $[Ir_2Rh_2(CO)_{11}PPh_3]$ [11]. The mole fractions of **5a** were determined as a function of time at nine temperatures (examples in *Fig. 2*) by measuring the integrals of the ^{31}P-NMR signals of the two isomers. The rate constants of the forward (k_1) and reverse (k_{-1}) isomerisation reactions, as well as the kinetic parameters, were then calcu-

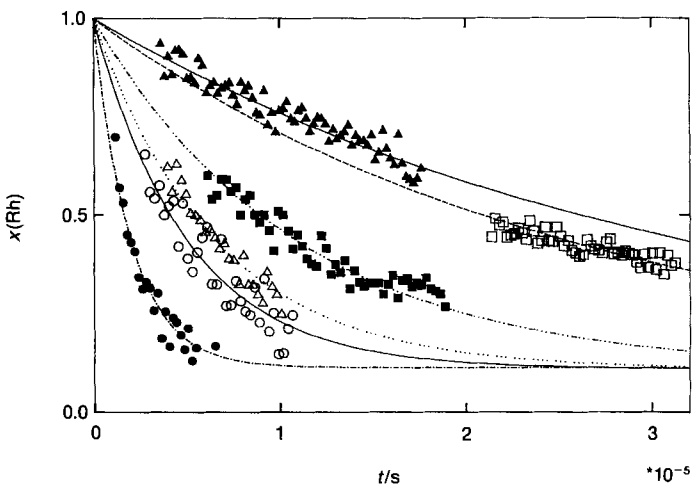

Fig. 2. *Mole fraction* (*x*) *of isomer* **5a** *as function of time* (*t*) *at six different temperatures.* △ = 293.0 K, □ = 294.7 K, ■ = 301.3 K, △ = 305.4 K, ○ = 307.6 K, ● = 315.5 K. The lines represent the calculated values using the parameters given in *Table 1*.

lated using the procedure described in [11]. The results are collected in *Table 1* where K is the ratio [**5b**]/[**5a**], $\Delta H_1^{\ddagger}$ and $\Delta S_1^{\ddagger}$ the activation parameters of reaction **5a** → **5b** and $\Delta G_{-1}^{\ddagger}$ that of the reverse reaction. The value of $\Delta G_{-1}^{\ddagger}$ has a larger error, because the contribution of the reverse reaction to the overall kinetics is small. The migration of PPh_3 in $[Ir_2Rh_2(CO)_{11}PPh_3]$ has a dissociative mode of activation as indicated by the positive values of the volumes of activation [11]. Assuming a similar mechanism for **5** and taking into account the statistical factors of 2/3 for k_1 and 2 for k_{-1}, the rate constants of interconversion of **5a** and **5b** are *ca.* 4 times greater than those of the Ir_2Rh_2 complex. This suggests that the strengths of the metal–P bonds are greater in the Ir_2Rh_2 than in the Ir_3Rh complex. This is in agreement with the results concerning the CO-scrambling processes (see below).

Table 1. *Kinetic Parameters and Equilibrium Constant for the Isomerisation* **5a** ⇌ **5b** *in* CD_2Cl_2 *at 298 K*

k_1 [s^{-1}]	k_{-1} [s^{-1}]	$\Delta H_1^{\ddagger}$ [kJ mol^{-1}]	$\Delta S_1^{\ddagger}$ [kJ mol^{-1}]	$\Delta G_1^{\ddagger}$ [kJ mol^{-1}]	K
$(6.5 \pm 0.1) \cdot 10^{-6}$	$(6.5 \pm 1.6) \cdot 10^{-7}$	92.1 ± 1.2	-37 ± 4	108 ± 25	8.5 ± 2

3. *Disubstituted Complexes.* The reaction of **2** with nbd or cod (1 mol-equiv.) in the presence of $AgBF_4$ in CH_2Cl_2 gave $[Ir_3Rh(CO)_{10}(\eta^4\text{-nbd})]$ (**6**; 75%) and $[Ir_3Rh(CO)_{10}(\eta^4\text{-cod})]$ (**7**; 65%), respectively. No CO substitution was observed under identical conditions when starting with $[Ir_4(CO)_{12}]$. Therefore, the site of substitution is the Rh-atom, as expected. The ^{13}C-NMR spectra of samples of **6** and **7** enriched in ^{13}CO in CD_2Cl_2 at 190 K are quite similar (see *Exper. Part*) and show that the ground-state geometry has C_s symmetry with 3 bridging CO's and with the diolefin chelating the basal Rh-atom (*Scheme 3*). A 2D-EXSY spectrum of **7** in CD_2Cl_2 at 243 K (mixing time: 100 ms) is presented in *Fig. 3* and shows the dynamic connectivities $a \leftrightarrow c$, $b \leftrightarrow g$, $c \leftrightarrow (a,e)$, and $d \leftrightarrow e$,

Scheme 3

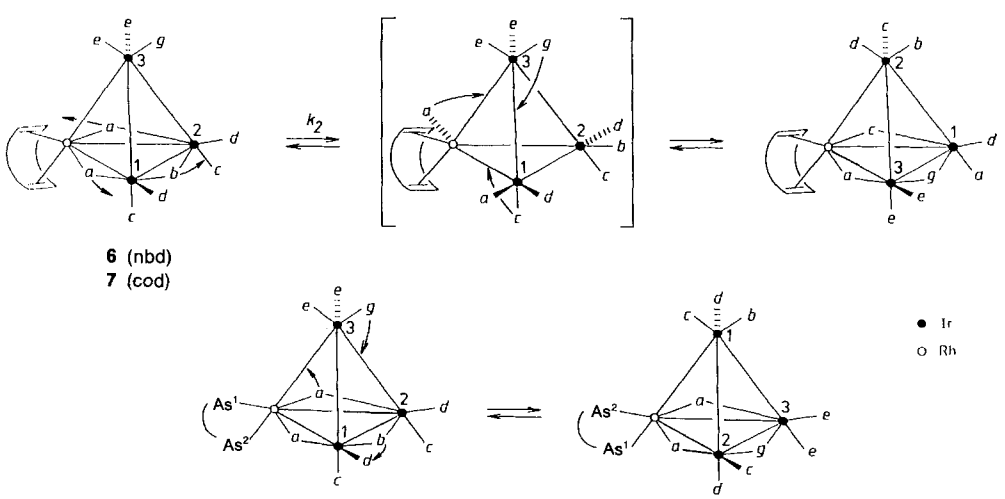

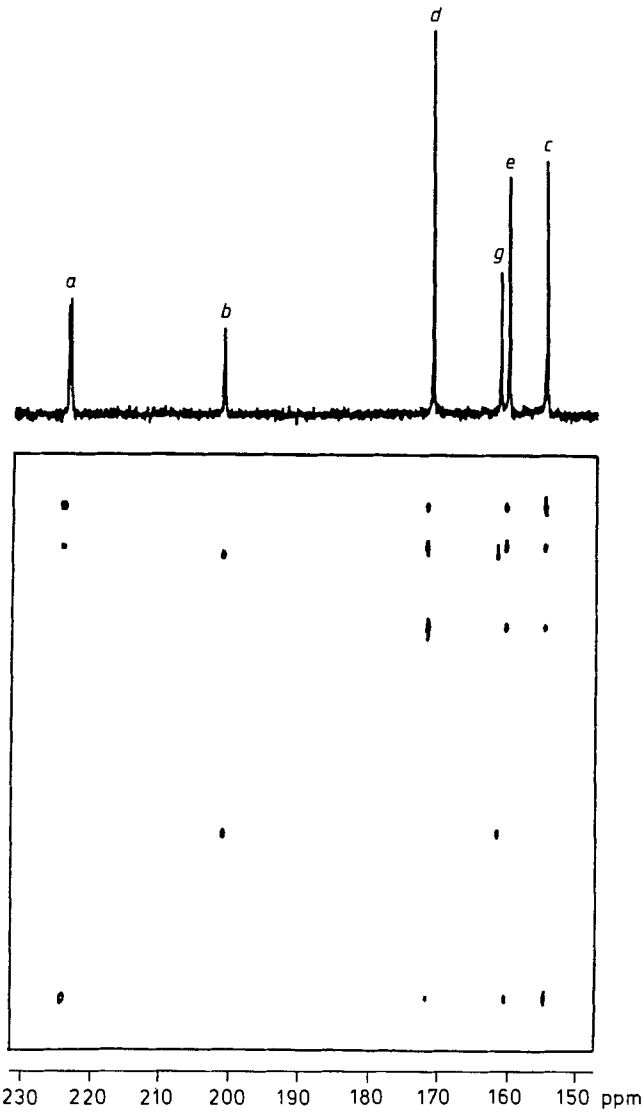

Fig. 3. *2D-EXSY ^{13}C-NMR Spectrum of [$Ir_3Rh(CO)_{10}(\eta^4$-cod)] (7) in CD_2Cl_2 at 243 K*

the other cross-peaks being second-order. Since apical-basal CO exchanges are observed including both types of μ_2-CO's, the scrambling process must be a change of basal face passing through an unbridged intermediate. A 2D-EXSY spectrum of **6** in CD_2Cl_2 at 200 K (mixing time: 100 ms) shows a single cross-peak between *e* and *g*. A second spectrum at 250 K (mixing time: 50 ms) establishes the same dynamic connectivities as for **7** taking into account the averaging of *e* and *g*. Therefore, the dynamic process with lowest activation energy in **6** is the rotation of apical CO's (rate constant k_1) and is followed by

the same change of basal face as for **7** (rate constant k_2, *Scheme 3*). Simulation of the variable-temperature ^{13}C-NMR spectra of **6** ($200 < T < 300$ K) using the exchange matrix elements $(a,a) = (d,d) = -k_2/2$, $(b,b) = (c,c) = -k_2$, $(b,g) = (g,b) = k_2$, $(a,c) = (c,a) = (c,e) = (e,c) = (d,e) = (e,d) = k_2/2$, $(g,g) = -k_2 \cdot -k_1$, $(e,e) = (-k_2 \cdot -k_1)/2$, $(g,e) = k_1$, and $(e,g) = k_1/2$, followed by *Eyring* regressions of $\ln(k/T)$ *vs.* $1/T$, gave the following free enthalpies of activation at 298 K: 49.4 ± 0.4 and 52.8 ± 0.8 kJ mol^{-1} for the rotation of apical CO's and the change of basal face, respectively. The change of basal face implies that the C=C bonds of the diolefin must swap positions. The ^{1}H-NMR spectrum of **6** in CD_2Cl_2 at 183 K presents two resonances corresponding to the pairs of olefinic protons in axial and radial positions. These broaden on raising the temperature and coalesce at *ca.* 303 K. Simulation of the variable-temperature ^{1}H-NMR spectra using a two site exchange matrix gave a $\Delta G^{\ddagger}$ of 53.1 ± 1.2 kJ mol^{-1} which is in good agreement with the value found for the change of basal face.

The reaction of **1** with 1 mol-equiv. of 1,2-phenylenebis(dimethylarsine) (= 1,2-bis(dimethylarsino)benzene; diars) in CH_2Cl_2 followed by chromatography gave [$Ir_3Rh(CO)_{10}(\eta^2$-diars)] (**8**; 56%). Its ground-state geometry in solution is similar to that of **6** and **7** as deduced from the ^{13}C-NMR spectrum of a sample enriched in ^{13}CO (see *Exper. Part*). A 2D-EXSY spectrum at 213 K (mixing time: 100 ms) shows the dynamic connectivities $b \leftrightarrow g$ and $c \leftrightarrow (e,d)$ (*Fig. 4*). Since apical-basal exchanges are observed and since the bridging CO *a* does not exchange, the site-exchange process must be a change of basal face (Rh–Ir(1)–Ir(2) and Rh–Ir(2)–Ir(3)). In contrast with **6** and **7**, this process must be synchronous, *e.g.*, it does not pass through an unbridged intermediate (*Scheme 3*). A successful simulation of the variable-temperature ^{13}C-NMR spectra was achieved using the exchange matrix elements $(b,g) = (g,b) = k$, $(c,d) = (d,c) = (d,e) = (e,d) = (c,e) = (e,c) = k/2$, and $(b,b) = (c,c) = (d,d) = (e,e) = (g,g) = -k$, where k = rate constant of the change of basal face (43 ± 3 at 200 K to 1753 ± 650 s^{-1} at 280 K). *Eyring* regression of $\ln(k/T)$ *vs.* $1/T$ gave a free enthalpy of activation of 52.3 ± 0.6 kJ mol^{-1} at 298 K. As for **6** an **7**, a consequence of the change of basal face is the positional exchange of the two $AsMe_2$ groups of the chelating ligand. This was confirmed by the variable-temperature ^{1}H-NMR spectra of **8** where the two Me signals (δ 1.80 and 1.32 at 177 K) coalesce into a *singlet* (δ 1.57) at 263 K. The rotation of apical CO's is not observed up to 300 K probably because of the greater steric hindrance caused by the $AsMe_2$ group in radial position relative to a C=C bond which is about parallel to the basal face (as show by the crystal structure of [$Ir_3Rh(CO)_8(\eta^4$-cod)$_2$] [6]). The values of the free enthalpy of activation of the change of basal face in [$Ir_4(CO)_{10}(\eta^4$-nbd)] (see *Exper. Part*) and [$Ir_4(CO)_{10}(\eta^2$-diars)] [12] are 36.3 ± 0.8 and 29.8 ± 0.6 kJ mol^{-1} at 298 K, respectively. Here again, substitution of Ir by Rh in the basal face increases the free enthalpy of activation of a concerted or non-concerted change of basal face by 16–22 kJ mol^{-1}.

The reaction of **4** with 1 mol-equiv. of methylenebis(diphenylphosphine) (= bis(diphenylphosphino)methane; dppm) followed by chromatography gave [$Ir_3Rh(CO)_7(\mu_2$-CO)$_3(\mu_2$-dppm)] (**9**; 56%). Its ^{31}P-NMR spectrum in (D_6)acetone at 183 K presents 3 signals with relative intensities 1:9:1 and with $\Delta\delta$'s corresponding to P-atoms in axial position. The major signal is a *singlet*. The minor ones show a P,P-coupling (40 Hz) and one of these has an additional P,Rh coupling (122 Hz) quite similar to that observed in [$Ir_2Rh_2(CO)_{10}(\mu_2$-dppm)]. The latter complex was synthesized by a similar

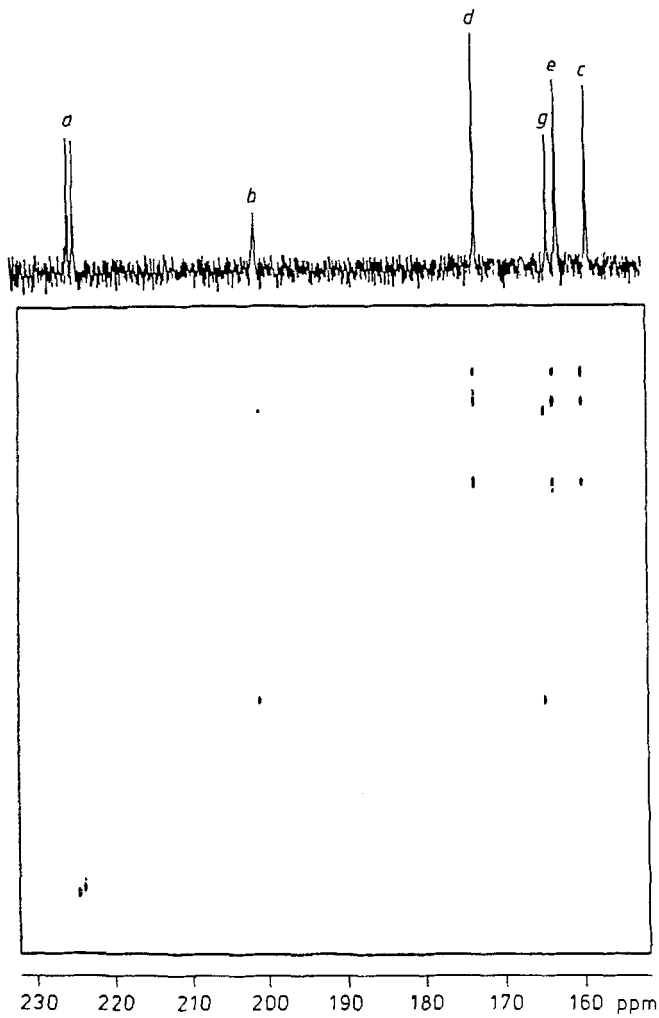

Fig. 4. *2D-EXSY* ^{13}*C-NMR Spectrum of* [$Ir_3Rh(CO)_{10}(\eta^2$-*diars*)] (**8**) *in* CD_2Cl_2 *at 213 K*

route starting with $[Ir_2Rh_2(CO)_{12}]$. Therefore, two isomers are present in solution. The bidentate ligand bridges two basal Ir-atoms in the major isomer **9a**, whereas it bridges one Ir- and the Rh-atom of the basal face in the minor isomers **9b**. The ^{13}C-NMR spectrum of a sample of **9** enriched in ^{13}CO (*ca.* 30%) in CD_2Cl_2 at 230 K (see *Exper. Part*) presents seven resonances with relative intensities 1:2:1:2:1:1:2 in order of decreasing δ's. The two resonances with highest δ's are characteristic of bridging CO's (*b*,*a*). A *doublet* (^1J(C,Rh) = 77 Hz) and a *singlet* with relative intensities 1:2 (*f*,*d*) have δ's in the region of radial CO's, and the resonance with lowest δ corresponds to an *AA'XX'* spin system indicating that two CO's (*g*) are in pseudo-*trans*-positions relative to a P-atom. These observations confirm that **9a** has C_s symmetry (see *Formula*). Ten minor resonances with equal relative intensities are also observed. Three of these have δ's in the region of the

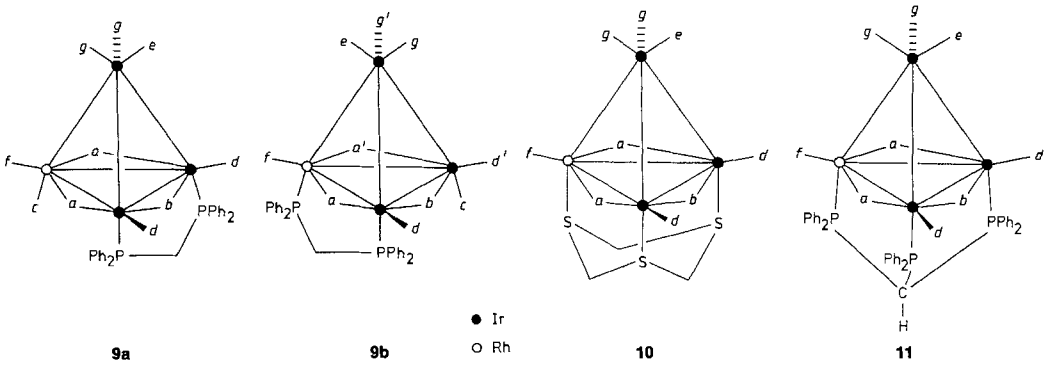

9a **9b** **10** **11**

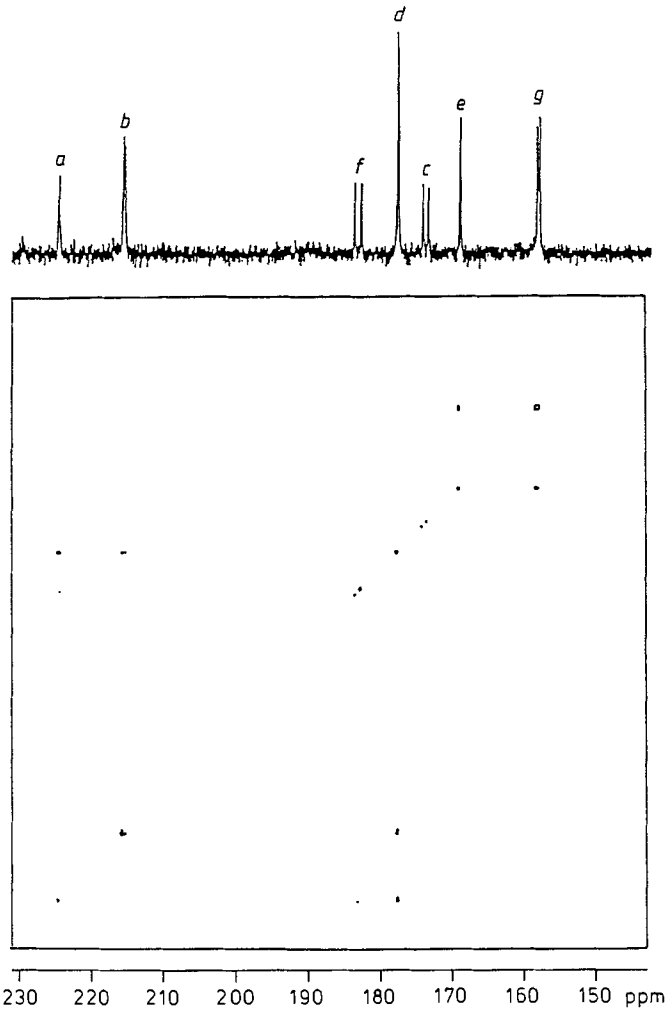

Fig. 5. *2D-EXSY ^{13}C-NMR Spectrum of [$Ir_3Rh(CO)_{10}(\mu_2$-dppm)]* (**9**) *in CD_2Cl_2 at 243 K*

bridging CO's and a resonance with δ typical for radial CO's shows a coupling with Rh (80 Hz) and a geminal coupling with P, in agreement with the geometry proposed for **9b**. A 2D-EXSY spectrum in CD_2Cl_2 at 243 K (mixing time 100 ms) shows for **9a** the dynamic connectivities $f \leftrightarrow a \leftrightarrow d \leftrightarrow b$, and $e \leftrightarrow g$ which correspond to the merry-go-round of 6 basal CO's and the rotation of 3 CO's about the apical Ir-atom, respectively (*Fig. 5*). The kinetics of isomerisation **9b** $\rightleftharpoons$ **9a** could not be followed as an equilibrium mixture of the two isomers was obtained during attempts to isolate the kinetically favoured isomer **9b**. It is, however, most probable that an intramolecular migration of one P-atom from Rh to Ir is responsible for the isomerisation of **9** and of $[Ir_2Rh_2(CO)_{10}(\mu_2$-dppm)].

4. *Trisubstituted Complexes.* The reaction of **3** with 1 mol-equiv. of 1,3,5-trithiane or methylidynetris(diphenylphosphine) (= tris(diphenylphosphino)methane; $CH(PPh_2)_3$) in the presence of $AgBF_4$ in THF yielded $[Ir_3Rh(CO)_6(\mu_2\text{-}CO)_3(\mu_3$-1,3,5-trithiane)] (**10**; 69%) and $[Ir_3Rh(CO)_6(\mu_2\text{-}CO)_3\{\mu_3\text{-}CH(PPh_2)_3\}]$ (**11**; 52%), respectively. The ^{13}C-NMR spectra of samples of **10** and **11** enriched in ^{13}CO are similar and present six resonances with relative intensities 2:1:1:2:1:2 in order of decreasing δ's (see *Exper. Part*). The first two pairs of signals have δ's in the region of bridging (*a,b*) and radial CO's (*f,d*), respectively. The ^{31}P-NMR spectrum of **11** in CD_2Cl_2 consists of a *doublet* of *triplets* due to P,Rh and P,P couplings and a *doublet* (^2J(P,P) = 31.4 Hz) with relative intensities 1:2. These observations indicate that **10** and **11** have C_s symmetry with the tridentate ligand capping the basal face (see *Formula*), in contrast to $[Rh_4(CO)_9(\mu_3$-trithiane)] which has a butterfly structure [13]. A 2D-EXSY spectrum of **10** at 210 K (mixing time 100 ms) shows the single exchange $e \leftrightarrow g$ corresponding to the rotation of apical CO's. A second spectrum at 240 K exhibits the additional exchange $a \leftrightarrow f \leftrightarrow d \leftrightarrow b$ due to the merry-go-round about the basal face. Simulation of the variable-temperature ^{13}C-NMR (*Fig. 6*) followed by *Eyring* regression gave values for $\Delta G^{\ddagger}$ (at 298 K) of 46.6 ± 0.4 (**10**) and 44.6 ± 0.4 (**11**) for the rotation of apical CO's, and 51.8 ± 0.4 (**10**) and 48.4 ± 0.5 kJ mol^{-1} (**11**) for the merry-go-round. These results, as well as those concerning **2** and **3**, show the necessity of referring to 2D-EXSY data to distinguish parallel, localised processes in cluster compounds from scrambling processes involving all metal atoms. The merry-go-round of the six basal CO's in $[Ir_4(CO)_6(\mu_2\text{-}CO)_3$(1,3,5-trithiane)] and $[Ir_2Rh_2(CO)_6(\mu_2\text{-}CO)_3$(1,3,5-trithiane)] have a $\Delta G^{\ddagger}$ (at 298 K) of 38.0 ± 0.5 [14] and > 68 kJ mol^{-1} [4], respectively. Therefore, substitution of Ir by Rh increases the activation energy of the merry-go-round. It was shown that the intermediate of the merry-go-round in the Ir_4 compound is the unbridged isomer [14]. Assuming the same type of intermediate for the isostructural mixed clusters, debridging of two Ir–Rh bonds in **10** requires *ca.* 15 kJ mol^{-1} more than debridging an Ir–Ir bond in the analogous Ir_4 compound. Debridging of a Rh–Rh bond in the Ir_2Rh_2 compound requires an additional 16 kJ mol^{-1} (or more) with respect to debridging an Ir–Ir bond in **10**.

$[Ir_3Rh(CO)_6(\mu_2\text{-}CO)_3(\eta^4$-nbd)$PPh_3]$ (**12**) is another example of a trisubstituted complex which was synthesized for the separation of **5a** and **5b** (*vide supra*). It exists as a single isomer in solution (see *Formula*) as deduced from its IR, ^{1}H-, ^{31}P-, and ^{13}C-NMR data (see *Exper. Part*). A single fluxional process takes place in solution leading to the coalescence of the signals *e*, *g*, and *g'*. Simulation of the variable-temperature ^{13}C-NMR spectra with the corresponding 3 site exchange matrix gave a free enthalpy of activation of 57.3 ± 0.4 kJ mol^{-1} at 298 K for the rotation of apical CO's at one metal centre.

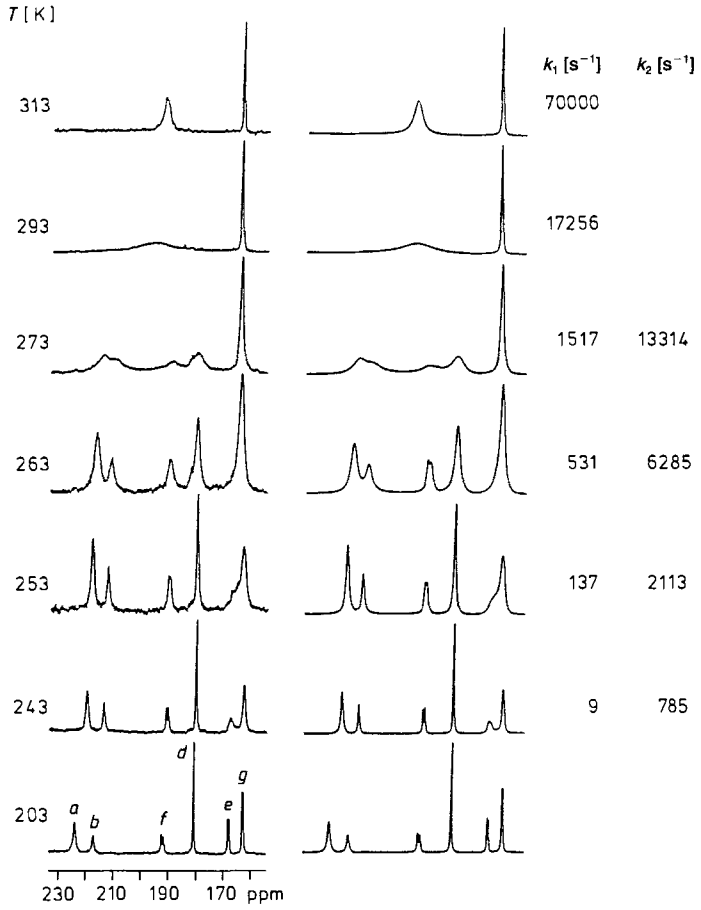

Fig. 6. *Experimental and calculated variable-temperature ^{13}C-NMR spectra of [$Ir_3Rh(CO)_9\{\mu_3$-$CH(PPh_2)_3\}$] (**11**) in (D_8)THF*

5. *Tetrasubstituted Complexes.* The reaction of **6** with excess diene in the presence of $Me_3NO \cdot 2\ H_2O$ followed by chromatography gave [$Ir_3Rh(CO)_8(\eta^4$-nbd)$_2$] (**13**). [$Ir_3Rh(CO)_8(\eta^4$-cod)(η^4-nbd)] (**14**) and [$Ir_3Rh(CO)_8(\eta^4$-cod)$_2$] (**15**) were obtained from [Ir(cod)Cl]$_2$ and [Rh(nbd)Cl]$_2$ in the presence of $AgPF_6$ in low yields (12–34%). The ^{13}C-NMR spectra of samples of **13**–**15** enriched in ^{13}CO are quite similar and present 8 resonances of equal intensities (see *Exper. Part*). Three of these (two *doublets* and one *singlet*) have δ's in the region of bridging CO's and one *singlet* is observed with δ in the region of radial CO's. Consequently, the diene ligands chelate the Rh- and an Ir-atom of the basal Ir_2Rh face, and their structure in solution are similar to that found in the solid state for **15** [6] (see *Formula*). As for **12**, the 2D-EXSY spectra (200 K and 150 ms, 223 K and 100 ms, and 280 K and 80 ms for **13**, **14**, and **15**, resp.) show the single dynamic connectivity $e \leftrightarrow g \leftrightarrow g'$. The variable-temperature ^{13}C-NMR spectra were simulated with the corresponding exchange matrix, and the results of *Eyring* regressions are shown in *Table 2*.

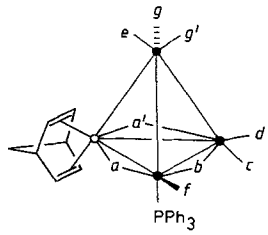

12

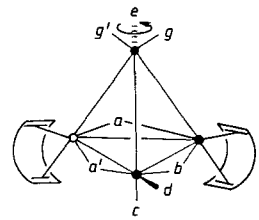

● Ir
○ Rh

13 $\eta^4 - L = \eta^4 - L' =$ nbd
14 $\eta^4 - L =$ nbd, $\eta^4 - L' =$ cod
15 $\eta^4 - L = \eta^4 - L' =$ cod

Table 2. *Free Enthalpy of Activation for the Rotation of Apical CO's* (298 K, CD_2Cl_2)

	$\Delta G^{\ddagger}$ [kJ mol^{-1}]		$\Delta G^{\ddagger}$ [kJ mol^{-1}]
$[Ir_4(CO)_8(\eta^4\text{-nbd})_2]$	46.7 ± 0.6	$[Ir_3Rh(CO)_8(\eta^4\text{-cod})_2]$ (**15**)	59.9 ± 0.3
$[Ir_4(CO)_8(\eta^4\text{-cod})(\eta^4\text{-nbd})]$	53.2 ± 0.2	$[Ir_2Rh_2(CO)_8(\eta^4\text{-nbd})_2]$	43.9 ± 0.6
$[Ir_4(CO)_8(\eta^4\text{-cod})_2]$	62.2 ± 0.2	$[Ir_2Rh_2(CO)_8(\eta^4\text{-cod})(\eta^4\text{-nbd})]$	46.7 ± 0.3
$[Ir_3Rh(CO)_8(\eta^4\text{-nbd})_2]$ (**13**)	43.0 ± 0.3	$[Ir_2Rh_2(CO)_8(\eta^4\text{-cod})_2]$	56.6 ± 0.3
$[Ir_3Rh(CO)_8(\eta^4\text{-cod})(\eta^4\text{-nbd})]$ (**14**)	50.5 ± 0.2		

To date, there is no information available on the factors affecting the activation barrier of the rotation of CO ligands at one metal centre in tetrahedral cluster compounds. Therefore, we undertook a similar kinetic study on the analogous $[Ir_2Rh_2(CO)_8(\eta^4\text{-diene})_2]$ complexes (see *Exper. Part*). The results are collected in *Table 2*, together with those concerning the corresponding Ir_4 clusters [15]. They indicate that substitution of Ir by Rh in the basal plane decreases the rotation barrier of CO's about the apical metal centre. The same trend is also observed when comparing the $\Delta G^{\ddagger}$'s of CO rotation in **6** (49.4 ± 0.4) and $[Ir_2Rh_2(CO)_{10}(\eta^4\text{-nbd})]$ (46.6 ± 0.6 [4]), in **10** (46.6 ● 0.4) and $[Ir_2Rh_2(CO)_9(\mu_2\text{-1,3,5-trithiane})]$ (42.0 ± 0.5 [4]), or in **11** (44.6 ± 0.4) and $[Ir_2Rh_2(CO)_9\{\mu_3\text{-}CH(PPh_2)_3\}]$ (41.0 ± 0.6 kJ mol^{-1} [4]). This suggests that some electron density in the Ir(apical)–M(basal) bonds is shifted towards the basal plane when M = Rh. Bridging CO's being better π-acceptors than terminal ones, the ground-state geometry with 3 μ_2-CO's should, therefore, be more stabilised relative to the unbridged one for mixed Ir–Rh clusters than for Ir_4 analogs. There are indeed no examples to date of Rh_4, $IrRh_3$, Ir_2Rh_2, and Ir_3Rh clusters with all CO's terminal, whereas several such examples are known for Ir_4 [16–18]. The mode of activation of the merry-go-round requires a shift between the μ_2- and the η_1-bonding modes of CO about the basal plane. The higher activation energies observed in the mixed clusters relative to the isostructural Ir_4 compounds are also in agreement with this view.

Another factor affecting the barrier of rotation of apical CO's is the steric hindrance caused by the ligands in radial position. For each series of clusters, the $\Delta G^{\ddagger}$ increases along the sequence $(nbd)_2 < (nbd)(cod) < (cod)_2$. Effectively, on replacing a 1,4- by a 1,5-diene, the olefinic C-atoms in radial position are relatively displaced from the mean basal plane towards the apical metal atom, as shown by a comparison between the crystal structures of $[Ir_2Rh_2(CO)_8(\eta^4\text{-nbd})]$ [4] and **14** [6].

Conclusion. – Substituted derivatives of $[Ir_3Rh(CO)_{12}]$ are fluxional in solution at the NMR time scale due to CO scrambling processes involving 1, 3, or 4 metal atoms. In one

case, an additional process takes place above room temperature: the intramolecular migration of PPh_3 from Rh to Ir. Substitution of Ir by Rh in the Ir_4 metal core slows all fluxional processes involving debridging of CO's: an increase of $\Delta G^{\ddagger}$ by *ca.* 15 kJ mol^{-1} is observed for the merry-go-round and by 15–22 kJ mol^{-1} for a change of basal face. In contrast, substitution of one or two Ir-atoms of the basal face by Rh lowers the $\Delta G^{\ddagger}$ of the rotation of apical CO's by *ca.* 3 to 5 kJ mol^{-1}. This can be explained by a shift of electron density towards the basal face in the ground-state geometry of Ir_3Rh and Ir_2Rh_2 cluster compounds relative to the Ir_4 analogs.

We thank the *Swiss National Science Foundation* for financial support and Dr. *G. Suardi* for the synthesis of $[Ir_2Rh_2(CO)_{10}(\mu^2\text{-dppm})]$.

Experimental Part

1. *General.* See [10]. Preparation of $[Ir_2Rh_2(CO)_8(\eta^4\text{-nbd})_2]$: see [4]. EXSY experiments: no decoupling, mixing times indicated in the text, typically 512 increments with 2 K transients, spectral width in both domains 8140 Hz, recorded for phase-sensitive representation. Before *Fourier* transformation, a square cosine bell was applied in both domains and the FID's were zero-filled to 2-K in the F_1 domain. The temperature was measured with a calibrated Pt-*100X* thermocouple, and stabilised using a *Bruker-VT-1000* unit.

2. *Dodecacarbonyltriiridiumrhodium* (**1**). A soln. of $[Ir(cod)Cl]_2$ (336 mg, 0.5 mmol), $[Rh(cod)Cl]_2$ (246.5 mg, 0.5 mmol), and $AgPF_6$ (506 mg, 2 mmol) in THF (30 ml) was stirred at 0° for 1 h, then filtered. The orange soln. was added dropwise under Ar to a soln. of $PPN[Ir(CO)_4]$ (1.7 g, 2 mmol; PPN = bis(triphenylphosphoranylidene)ammonium) in THF (100 ml)/pentane (30 ml) and stirred at −50° for 1 h. Pentane (50 ml) was added and the mixture allowed to warm to r.t. and filtered on silica gel. Evaporation left a red residue (990 mg) which was dissolved in CH_2Cl_2/hexane (80 ml), stirred under CO (1 atm) at r.t. for 10 h, and filtered giving a yellow-orange precipitate of **1** contaminated by $[Ir_4(CO)_{12}]$. The filtrate was chromatographed (silica gel) giving pure **1** (150 mg) as orange microcrystals. The precipitate was reacted with bicyclo[2.2.1]hepta-2,5-diene (= norbornadiene; nbd; 5 ml) in refluxing THF (50 ml) for 12 h. Unreacted $[Ir_4(CO)_{12}]$ was filtered off and the filtrate evaporated. The residue was stirred in CH_2Cl_2/hexane 1:1 (80 ml) under CO (1 atm). After 10 h, an additional crop of **1** was filtered (180 mg). Overall yield: 34%. IR (THF): 2067*vs*, 2029*s*, 1990*w*, 1880*m*, 1848*m*. IR (nujol): 2057*vs* (br., CO). EI-MS (70 eV): 1018 (13, M^+), 990, 962, 934, 906, 878, 850 (each 13), 822 (48), 794 (63), 766 (58), 738 (59), 707 (54), 679 (100), 576 (20, Ir_3), 487 (32, Ir_2Rh), 384 (28, Ir_2); the envelope of the molecular peak is in agreement with the relative populations of the 4 isotopomers of Ir_3Rh; the reported m/z (> 679) correspond to the isotopomer $^{193}Ir_3Rh$ and show the successive losses of 12 CO. Anal. calc. for $C_{12}H_3Ir_3O_{12}Rh$ (1015.7): C 14.19, Ir + Rh 66.91; found: C 14.02, Ir + Rh 66.65.

3. *Substituted Derivatives of* **1**. *Tetraethylammonium Undecacarbonyliodotriiridiumrhodate(1−)* (**2**) *and Tetraethylammonium Bromoundecacarbonyltriiridiumrhodate(1−)* (**3**). A suspension of **1** (365 mg, 0.36 mmol) and $[NEt_4]I$ (185 mg, 0.72 mmol) or $[NEt_4]Br$ (0.72 mmol) in THF (50 ml) was stirred under Ar at 40° for 10 h. Evaporation and crystallisation of the residue from THF/MeOH at −25° gave microcrystals of **2** (red, 70%) and **3** (orange, 64%).

Data of **2**: IR (CH_2Cl_2): 2075*m*, 2065*m*, 2044*s*, 2005*s*, 1895*vw*, 1844*m* (CO). ^{13}C-NMR ((D_8)THF, 203 K): 221.6 (*dt*, J(C,C) = 8, J(C,Rh) = 32.4, *a*); 203.9 (*t*, J(C,C) = 8, *b*); 187.0 (*d*, J(C,Rh) = 79.5, *f*); 173.3, 165.9, 160.6, 155.7 (4*s*, *d*, *g*, *e*, *c*); rel. intensities 2:1:1:2:1:2:2. 2D-COSY (F = 3802 Hz, (D_8)THF, 210 K): cross-peak between 160.6 and 155.7 (CO's in pseudo-*trans*-positions). Simulation of VT-^{13}C-NMR (T[K], k_1[s^{-1}], k_2[s^{-1}]): 223, 12, 0; 233, 30, 4; 243, 63, 8; 253, 138, 39; 263, 327, 177; 273, 798, 625; 283, 1827, 1297; 293, 350, 3210. Anal. calc. for $C_{19}H_{20}Ir_3NO_{11}Rh$ (1244.8): C 18.33, H 1.62, N 1.13; found: C 18.45, H 1.76, N 1.23.

Data of **3**: Complex **3** is thermally less stable than **2**. IR (acetone): 2079*m*, 2047*s*, 2007*s*, 1896*vw*, 1836*m* (CO). ^{13}C-NMR ((D_8)THF, 203 K): 224.7 (*dt*, J(C,C) = 8, J(C,Rh) = 32.1, *a*); 204.8 (*t*, J(C,C) = 8, *b*); 186.1 (*d*, J(C,Rh) = 80.3, *f*); 173.7, 165.3, 159.9, 156.1 (4*s*, *d*, *g*, *e*, *c*); rel. intensities as for **2**. Simulation of VT-^{13}C-NMR (T[K], k_1[s^{-1}], k_2[s^{-1}]): 248, 71, 141; 253, 119, 213; 258, 234, 376; 263, 385, 491; 268, 501, 696; 273, 828, 991. Anal. calc. for $C_{19}H_{20}BrIr_3NO_{11}Rh$ (1197.8): C 19.05, H 1.68, N 1.17; found: C 19.14, H 1.81, N 1.23.

[(2,3-η)-Bicyclo[2.2.1]hept-2-ene]undecacarbonyltriiridiumrhodium (**4**). A soln. of **2** (0.25 mmol), bicyclo[2.2.1]hept-2-ene (0.25 mmol), and $AgClO_4$ (2 mmol) in CH_2Cl_2 (50 ml) was stirred at −50° for 2 h. Filtration

and evaporation at 0° gave a residue which could not be recrystallised without decomposition, but could be dissolved in CD_2Cl_2. ^{1}H-NMR (200 K): 4.42 (*s*, H–C(2), H–C(3)); 2.81 (*s*, H–C(1), H–C(4)); 1.45, 0.78 (2*m*, 2 H each, CH_2(5), CH_2(6)); 1.13 (*s*, CH_2(7)). ^{13}C-NMR (233 K): 217.5 (*d*, *J*(C,Rh) = 29.1, *a*); 199.5 (*s*, *b*); 181.9 (*d*, *J*(C,Rh) = 78.5, *f*; 170.7, 164.1, 157.6, 155.4 (4*s*, *d*, *g*, *e*, *c*); rel. intensities as for **2**. 2D-COSY (183 K): cross-peak between 217.5 and 199.5 and between 157.6 and 155.4. Simulation of VT-^{13}C-NMR (*T*[K], k_1[s^{-1}], k_2[s^{-1}]): 223, 36, 0; 233, 45, 0; 243, 60, 15; 253, 112, 39; 263, 189, 126; 273, 324, 362; 283, 437, 743.

Undecacarbonyl(triphenylphosphine)triiridiumrhodium (**5**). A soln. of **4** (0.45 mmol) and PPh_3 (132 mg, 0.5 mmol) in THF (50 ml) was stirred at −10° for 2 h. Evaporation to a small volume and chromatography (*Lobar*, silica gel, CH_2Cl_2/hexane 1:2) gave **5** (326 mg, 58%). Yellow microcrystals. IR (CH_2Cl_2): 2076*m*, 2051*s*, 2016*s*, 1984*m*, 1845*m*, 1826*m*, 1810*m* (CO). ^{31}P-NMR (CD_2Cl_2, r.t., 85% H_3PO_4 as external reference): −10.1 (*s*, $\Delta\delta = \delta_{Pcoord} - \delta_{Pfree} = -5.3$); 8.9 (*d*, *J*(P,Rh) = 122.2, $\Delta\delta$ = +13.7). Anal. calc. for $C_{29}H_{15}Ir_3O_{11}PRh$ (1250.0): C 27.87, H 1.21, P 2.48; found: C 27.59, H 1.34, P 2.30.

The same reaction effected directly in a NMR tube showed the formation of the kinetically favoured isomer **5a**. ^{13}C-NMR (CD_2Cl_2, 250 K): 215.5 (*dd*, *J*(C,Rh) = 32, *J*(C,P) = 6, *a*); 198.3 (*t*, *J*(C,P) = 9.1, *b*); 183.7 (*dd*, *J*(C,Rh) = 78.0, *J*(C,P) = 6.4, *f*); 169.7 (*s*, *d*); 164.2 (*d*, *J*(C,P) = 32, *g*); 159.6, 157.3 (2*s*, *e*, *c*); intensities 2:1:1:2:1:2:2. 2D-COSY: cross-peaks between *a* and *b*, *f* and *d*, and *e* and *c*. On warming the soln. at 313 K, a gradual decrease in intensity of the ^{31}P- and ^{13}C-NMR signals (spectra of samples taken after rapid cooling to 213 K) due to **5a** was observed together with a gradual increase in intensity of signals attributed to the thermodynamically favoured isomer **5b**.

Isomer **5b** was obtained by reacting **5a**/**5b** with nbd (1 mol-equiv.) in refluxing CH_2Cl for 4 h, giving **12** and unreacted **5a** which were separated by chromatography (see below) then the soln. of **12** in CH_2Cl_2 was stirred under CO (1 atm) at r.t. for 12 h. Evaporation and crystallisation from CH_2Cl_2/hexane at −25° gave **5b** (88%). ^{13}C-NMR (CD_2Cl_2, 170 K): 216.6 (*dd*, *J*(C,Rh) = 24, *J*(C,P) = 6, *a*); 207.9 (*d*, *J*(C,Rh) = 25, *a'*); 207.5 (*d*, *J*(C,P) = 6, *b*); 180.5 (*d*, *J*(C,Rh) = 75, *d'*); 171.0 (*d*, *J*(C,P) = 13, *f*); 169.5 (*s*, *d*); 169.4 (*d*, *J*(C,Rh) = 64, *c'*); 166.0, 159.2, 157.6 (3*s*, *e'*, *e*, *c*); 157.6 (*d*, *J*(C,P) = 26, *g*). 2D-COSY: cross-peaks between *a*, *a'* and *b*, *c*, and *e* (pseudo-*trans*), *c'* and *e'* (pseudo-*trans*), and *d'*, *f* and *d* (pseudo-*cis*).

[(2,3-η:5,6-η)-Bicyclo[2.2.1]hepta-2,5-diene]decacarbonyltriiridiumrhodium (**6**) *and Decacarbonyl[(1,2-η:5,6-η)-cycloocta-1,5-diene]triiridiumrhodium* (**7**). A suspension of **1** (132 mg, 0.13 mmol) and nbd (0.14 ml, 1.3 mmol) or cod (20 mg, 0.18 mmol) in CH_2Cl_2 (50 ml) was refluxed for 4 h (nbd) or stirred at 40° for 2 h (cod; TLC monitoring). After evaporation, the residue was extracted into CH_2Cl_2 and purified by column chromatography (*Lobar B*, *Lichroprop Si 60*, 40–63 μm, CH_2Cl_2/hexane 1:2). The 1st fraction gave **6** (orange microcrystals; 102 mg, 75%) or **7** (red crystals; 91 mg, 65%) after recrystallisation from CH_2Cl_2/hexane at −25°. In the case of cod, a 2nd fraction contained **15**.

Data of **6**: IR (CH_2Cl_2): 2078*s*, 2051v*s*, 2016*s*, 1880*w*, 1840 (br.), 1815*m* (CO). ^{1}H-NMR (CD_2Cl_2, 183 K): 4.95, 4.47 (2*s*, H–C(2), H–C(3), H–C(5), H–C(6)); 4.12 (*s*, H–C(1), H–C(4)); 1.13 (*m*, CH_2(7)); the *s* at 4.95 and 4.47 coalesce at 303 K. ^{13}C-NMR (CD_2Cl_2, 210 K): 221.1 (*dd*, *J*(C,Rh) = 27, *J*(C,C) = 8, *a*); 203.3 (*t*, *J*(C,C) = 8, *b*); 170.8, 161.6, 161.1, 153.6 (4*s*, *d*, *g*, *e*, *c*); rel. intensities 2:1:2:1:2:2. Simulation of VT-^{13}C-NMR (*T*[K], k_1[s^{-1}], k_2[s^{-1}]): 215, 28, 0; 220, 38, 0; 225, 75, 0; 230, 122, 0; 235, 184, 0; 240, 294, 0; 250, 596, 40; 260, 1248, 99; 265, –, 146; 270, 2541, 247; 275, –, 320; 280, 4856, 594; 290, 8822, 2118; 300, 15420 (extrapolated), 4964. Simulation of VT-^{1}H-NMR (*T*[K], *k* [s^{-1}]): 243, 10.1; 253, 29.9; 263, 99; 273, 360; 283, 1109; 293, 2600; 303, 6809. Anal. calc. for $C_{17}H_8Ir_3O_{10}Rh$ (1051.8): C 19.41, H 0.77; found: C 19.36, H 0.81.

Dato of **7**: IR (CH_2Cl_2): 2080*s*, 2050v*s*, 2014*s*, 1985*m*, 1880*w*, 1837*s*, 1815*m* (CO). ^{1}H-NMR (CD_2Cl_2, 230 K): 4.72, 3.70, 2.96, 2.56, 2.30, 1.81 (6*m*). ^{13}C-NMR (CD_2Cl_2, 230 K): 223.9 (*d*, *J*(C,Rh) = 28, *a*); 200.8 (*s*, *b*); 171.9, 161.9, 160.8, 155.1 (4*s*, *d*, *g*, *e*, *c*); rel. intensities as for **6**. Anal. calc. for $C_{18}H_{12}Ir_3O_{10}Rh$ (1067.8): C 20.25, H 1.13, Ir + Rh 63.54; found: C 20.34, H 1.08, Ir + Rh 63.45.

Decarbonyl[1,2-phenylenebis(dimethylarsine)-K^{2}As,As']triiridiumrhodium (**8**). A suspension of **1** (152 mg, 0.15 mmol) and 1,2-phenylenebis(dimethylarsine) (43 μl, 0.15 mmol) in CH_2Cl_2 (50 ml) was stirred at r.t. for 8 h under Ar. After filtration of an unidentified brown powder, the soln. was evaporated and the residue purified column chromatography (same conditions as for **6**) and recrystallisation from CH_2Cl_2/hexane at −25°: **8** (104 mg, 56%). Red. microcrystals. IR (CH_2Cl_2): 2056*s*, 2025v*s*, 1995*s*, 1962*w*, 1815*m*, 1787*m* (CO). ^{1}H-NMR (CD_2Cl_2, 177 K): 7.81 (*m*, 4 arom. H); 1.80, 1.32 (2*s*, 4 Me); 2*s* coalesce at 263 K. ^{13}C-NMR (CD_2Cl_2, 173 K): 225.5 (*dd*, *J*(C,Rh) = 35, *J*(C,C) = 8, *a*); 201.9 (*t*, *J*(C,C) = 7, *b*); 173.1, 163.9 (2*s*, *d*, *g*); 162.7, 158.7 (2'*t*', *J*(C,C) = 5, *e*, *c*); rel. intensities 2:1:2:1:2:2. Simulation of VT-^{13}C-NMR (*T*[K], k_1[s^{-1}]): 200, 43; 210, 67; 220, 111; 230, 253; 240, 543; 260, 1300; 280, 1753. Anal. calc. for $C_{20}H_{16}As_2Ir_3O_{10}Rh$ (1245.7): C 19.28, H 1.29, As 12.03; found: C 19.17, H 1.20, As 12.31.

Decarbonyl[μ_2-methylenebis(diphenylphosphine)-K^2P,P′]triiridiumrhodium (**9**). A soln. of **4** (0.25 mmol) and methylenebis(diphenylphosphine) (96 mg, 0.25 mmol) was stirred at r.t. for 2 h, then evaporated to a small volume. Column chromatography (*Lobar B, Lichroprop Si 60*, 40–63 μm, CH_2Cl_2/hexane 1:1) and recrystallisation from CH_2Cl_2/hexane at −25° gave **9** (187 mg, 56%). IR (THF): 2066*s*, 2035*s*, 2006*vs*, 1958*vw*, 1870*w*, 1842*vw*, 1789*m* (CO). ^{31}P-NMR ((D$_6$)acetone, 183 K): −28.5 (*dd*, J(P,Rh) = 122, J(P,P) = 40, $\Delta\delta$ = −6, **9b**): −43.1 (*s*, $\Delta\delta$ = −20.6, **9a**); −45.7 (*d*, J(P,P) = 40, $\Delta\delta$ = −23.2, **9b**); rel. intensities 1:9:1. ^{13}C-NMR (CD_2Cl_2, 203 K): **9a**: 224.7 (*s*, *b*); 215.8 (*d*, J(C,Rh) = 20, *a*); 182.9 (*d*, J(C,Rh) = 77, *f*); 177.6 (*d*, J(C,P) = 4, *d*); 173.5 (*d*, J(C,Rh) = 66, *c*); 169.5 (*s*, *e*); 158.6 (*m*, *g*); rel. intensities 1:2:1:2:1:1:2; **9b**: 229.3, 216.8 (2*d*, J(C,Rh); 22, *a*, *a*′); 207.1 (*s*, *b*); 189.6 (*dd*, J(C,Rh) = 80, J(C,P) = 9, *f*); 177.7 (*d*, J(C,P) = 4, *d*); 170.5 (*s*, *d*′); 165.5, 159.4 (2*d*, J(C,P) = 44, 42, *g*′, *g*); 163.9, 162.6 (2*s*, *e*, *c*). Anal. calc. for $C_{35}H_{22}Ir_3O_{10}P_2Rh$ (1344.1): C 31.18, H 1.65, P 4.61; found: C 30.98, H 1.54, P 4.51.

Nonacarbonyl(μ_3-1,3,5-trithiane-K^3S^1,S^3,S^5)triiridiumrhodium (**10**). A soln. of **2** (201 mg, 0.16 mmol), $AgBF_4$ (62 mg, 0.3 mmol), and 1,3,5-trithiane (35 mg, 0.25 mmol) in THF (20 ml) was stirred at −20° for 1 h, filtered, and then refluxed for 2 h (TLC monitoring). The red soln. was evaporated to a small volume and chromatographed (same conditions as for **6**): $[Ir_3Rh(CO)_{10}\{\mu_2$-(1,3,5-trithiane)$\}]$ (14 mg, 8%) and then **10** (118 mg, 69%), as red microcrystals. **10**: IR (THF): 2065*w*, 2015*m*, 2007*m*, 1963*s*, 1852*vw*, 1815*m* (CO). ^{1}H-NMR (CD_2Cl_2, 173 K): 4.75, 3.51, 2.83 (3*m*, 2 H each). ^{13}C-NMR (CD_2Cl_2, 191 K): 242.7 (*dd*, J(C,Rh) = 25, J(C,C) = 12, *a*); 233.7 (*t*, J(C,C) = 9, *b*); 190.3 (*d*, J(C,Rh) = 80, *f*); 179.6, 167.1, 161.8 (3*s*, *d*, *e*, *g*); rel. intensities 2:1:1:2:1:2. Simulation of VT-^{13}C-NMR (T[K], k_1[s^{-1}], k_2[s^{-1}]): 213, 25, 0; 223, 78, 0; 228, 218, 0; 233, 315, 0; 243, 773, 0; 248, 1536, 78; 253; –, 101; 258, 1973, 158; 263, –, 271; 268, 4984, 467; 293, 29516, 3745; 303, 51609 (extrapolated), 6609; 313, –, 15560; 323, –, 31015. Anal. calc. for $C_{12}H_6Ir_3O_9RhS_3$ (1069.9): C 13.47, H 0.57, S 8.99; found: C 13.69, H 0.80, S 8.95.

Nonacarbonyl[μ_3-methylidenetris(diphenylphospine)-K^3,P,P′,P″]triiridiumrhodium (**11**). A soln. of **2** (186 mg, 0.15 mmol), $AgClO_4$ (0.3 mmol), and methylidynetris(diphenylphosphine) (136 mg, 0.25 mmol) was stirred at −15° for 15 min, filtered, and then heated at 60° for 10 h (TLC monitoring). After evaporation, the residue was extracted into CH_2Cl_2 and chromatographed (same conditions as for **6**): orange, unidentified product (5 mg) and then, after recrystallisation from CH_2Cl_2/hexane at −20°, **11** (113 mg, 50%). IR (CH_2Cl_2): 2056*s*, 2002*vs*, 1983*m*, 1807*m*, 1779*m* (CO). ^{31}P-NMR (CD_2Cl_2, r.t.): −18.1 (*dt*, J(P,Rh) = 127.6, ^2J(P,P) = 30, $\Delta\delta$ = 7.4, 1 P); −30.9 (*d*, J(P,Ph) = 31, $\Delta\delta$ = −5.4, 2 P). ^{13}C-NMR ((D$_8$)THF, 183 K): 228.3 (*d*, J(C,Rh) = 24, *a*); 221.1 (*s*, *b*); 193.0 (*d*, J(C,Rh) = 79, *f*); 180.6 (*s*, *d*); 166.5 (*d*, J(C,P) = 49, *e*); 161.0 (*m*, *g*); rel. intensities 2:1:1:2:1:2.

[(2,3-η:5,6-η)-Bicyclo[2.2.1]hepta-2,5-diene]nonacarbonyl(triphenylphosphine)triiridiumrhodium (**12**). A soln. of **5a**/**5b** (160 mg, 0.13 mmol) and nbd (28 μl, 0.27 mmol) in CH_2Cl_2 (50 ml) was refluxed for 4 h. Evaporation to a small volume, filtration, and chromatography (*Lobar B, Lichroprep Si 60*, 40–63 μm, CH_2Cl_2/hexane 1:4) gave first **5a** and then, after recrystallisation from CH_2Cl_2/hexane 1:4 at −25°, **12** (77 mg, 46%). Red crystals. IR (CH_2Cl_2): 2051*s*, 2021*vs*, 1973*m*, 1830*m*, 1808*s* (CO). ^{1}H-NMR (CD_2Cl_2, 303 K): 7.54, 7.12 (2*m*, Ph); 4.79, 4.46, 4.18, 4.05, 3.82, 3.21 (6*s*, 6 H); 1.40 (*m*, CH_2(7)). ^{13}C-NMR ((D$_8$)THF, 200 K): 230.4, 221.5 (2*d*, J(C,Rh) = 31, 34, *a*, *a*′); 211.7 (*s*, *b*); 173.9 (*d*, J(C,P) = 3, *f*); 170.9, 164.1, 163.4 (3*s*, *d*, *g*, *g*′); 161.6 (*d*, J(C,P) = 36, *e*); 160.3 (*s*, *c*). Simulation of VT-^{13}C-NMR (T[K], k[s^{-1}]): 240, 11; 250, 15,8; 260, 39; 270, 79; 290, 430; 300, 658. Anal. calc. for $C_{34}H_{23}Ir_3O_9PRh$ (1286.1): C 31.75, H 1.80, P 2.41; found: C 31.89, H 1.71, P 2.69.

Bis[(2,3-η:5,6-η)-bicyclo[2.2.1]hepta-2,5-diene]octacarbonyltriiridiumrhodium (**13**). A soln. of **6** (106 mg, 0.1 mmol), nbd (108 μl, 1 mmol), and $Me_3NO \cdot 2\,H_2O$ (105 mg) was stirred at −10° for 2 h (TLC (CH_2Cl_2/hexane 1:2) monitoring). Filtration and evaporation left a residue which was extracted into CH_2Cl_2 and chromatographed (same conditions as for **6**): red **13** (30 mg, 28%), after recrystallisation from CH_2Cl_2/hexane at −25°. IR (THF): 2051*s*, 2023*s*, 1983*m*, 1947*w*, 1821*s*, 1804*s*, 1774*m* (CO). ^{1}H-NMR (CD_2Cl_2, 243 K): 5.01, 4.84, 4.79, 4.50, 4.47, 4.42, 4.22, 4.04, 3.87, 3.79 (12 H); 1.87, 1.31, 1.29, 1.21 (4*m*, 4 H). ^{13}C-NMR (CD_2Cl_2, 190 K): 233.5, 225.0 (2*d*, J(C,Rh) = 31, 29, *a*, *a*′); 215.5, 172.8, 164.9, 164.6, 158.5, 155.0 (6*s*, *b*, *d*, *e*, *g*, *g*′, *c*). 2D-COSY (F = 7650 Hz): cross-peak between 164.9 and 155.0 (pseudo-*trans*). Simulation of VT-^{13}C-NMR (T[*K*], k_1[s^{-1}]): 200, 49; 210, 150; 220, 468; 230, 1287; 240, 3487; 250, 5464; 260, 12056. Anal. calc. for $C_{22}H_{16}Ir_3O_8Rh$ (1087.9): C 24.29, H 1.48; found: C 24.10, H 1.51.

[(2,3-η;5,6-η)-Bicyclo[2.2.1]hepta-2,5-diene]octacarbonyl[(1,2-η:5,6-η)-cycloocta-1,5-diene]triiridiumrhodium (**14**). A soln. of $[Ir(cod)Cl]_2$ (335 mg, 0.5 mmol), $[Rh(nbd)Cl]_2$ (230 mg, 0.5 mmol), and $AgPF_6$ (506 mg, 2 mmol) in THF (20 ml) was stirred at −20° for 1 h, then filtered. The resulting yellow soln. was added dropwise to a soln. of PPN[Ir(CO)$_4$] (1.69 g, 2 mmol) in THF (50 ml)/pentane (20 ml) and stirred at −50° for 1 h. Pentane (50 ml) was added. Filtration and chromatography (*Lobar B, Lichroprop Si 60*, 40–63 μm, CH_2Cl_2/hexane 1:3) gave $[Ir_3Rh(CO)_8(nbd)_2]$ (82 mg), **14** (134 mg, 12%), and **15** (40 mg). **14**: IR (THF): 2053*s*, 2030*vs*, 1988*s*, 1950*w*, 1824*s*, 1804*s*, 1774*m* (CO). ^{1}H-NMR (CD_2Cl_2, 220 K): 5.01, 4.86, 4.57, 4.51, 4.24, 4.09, 1.37 (8 H, nbd); 4.5, 4.4, 3.4, 3.0, 2.7, 2.4, 2.0, 1.8 (12 H). ^{13}C-NMR (CD_2Cl_2, 173 K): 234.6, 224.6 (2*d*, J(C,Rh) = 26, 27, *a*, *a*′); 217.8, 175.9, 164.5,

164.4, 160.0, 156.9 (6*s*, *b*, *d*, *e*, *g*, *g'*, *c*). 2D-COSY (F = 1930 Hz): cross-peak between 164.4 and 156.9 (pseudo-*trans*). Simulation of VT-^{13}C-NMR (T[K], k_1[s^{-1}]): 213, 12; 223, 33; 233, 82; 243, 192; 253, 418; 263, 859; 273, 1986; 293, 6954. Anal. calc. for $C_{23}H_{20}Ir_3O_8Rh$ (1104.0): C 25.02, H 1.83; found: C 24.85, H 1.97.

Octacarbonyl[(1,2-η:5,6-η)-cycloocta-1,5-diene]triiridiumrhodium (**15**). Preparation, crystal structure, and ^{13}C-NMR data: see [6]. IR (THF): 2049*s*, 2026*vs*, 1993*s*, 1966*w*, 1823*s*, 1795*s*, 1770*m* (CO). Anal. calc. for $C_{24}H_{24}Ir_3O_8Rh$ (1120.0): C 25.74, H 2.16; found: C 25.99, H 2.04.

4. *Substituted Derivatives of [$Ir_2Rh_2(CO)_{12}$]. Bis[(2,3-η:5,6-η)-bicyclo[2.2.1]hept-2,5-diene]octacarbonyldiiridiumdirhodium.* Preparation, crystal structure, and ^{13}C-NMR data: see [4]. ^{13}C-NMR (CD_2Cl_2, 190 K)[3]): 248.5 (*t*, J(C,Rh) = 32, *a*); 227.9 (*d*, J(C,Rh) = 29, *b*); 172.2, 170.0, 166.6, 157.2 (4*s*, *d*, *e*, *g*, *c*); rel. intensities 1:2:1:1:2:1. 2D-COSY: cross-peaks between *e* and *c*. Simulation of VT-^{13}C-NMR (T[K], k[s^{-1}]): 180, 5; 185, 32; 200, 196; 210, 447; 220, 936.

[(2,3-η:5,6-η)-Bicyclo[2.2.1]hepta-2,5-diene]octacarbonyl[(1,2-η:5,5-η)-cyclocta-1,5-diene]diiridiumdirhodium. As described for **14** but using 1 mmol of $[Ir(CO)_4]^-$. Yield: 12%. IR (CH_2Cl_2): 2052*s*, 2025*vs*, 1990*s*, 1950*w*, 1818*s* (CO). ^{13}C-NMR (CD_2Cl_2, 170 K): 249.5 (*t*, J(C,Rh) = 31, *a*); 230.2, 226.6 (2*d*, J(C,Rh) = 29, *b*, *b'*); 172.8, 166.7, 166.5, 166.2, 158.5 (5*s*, *d*, *e*, *g*, *g'*, *c*). Simulation of VT-^{13}C-NMR (T[K], k[s^{-1}]): 190, 8; 195, 15; 200, 30; 205, 50; 210, 71, 220, 190. Anal. calc. for $C_{23}H_{20}Ir_2O_8Rh_2$ (1014.7): C 27.22, H 1.99; found: C 27.85, H 1.97.

Octacarbonylbis[(1,2-η:5,6-η)-cycloocta-1,5-diene]diiridiumdirhodium. A soln. of [$Ir_2Rh_2(CO)_{12}$] (580 mg, 0.62 mmol) and cod (338 mg, 3.1 mmol) in CH_2Cl_2 (55 ml) was stirred at 50° for 12 h. (TLC monitoring). After evaporation, the residue was extracted into CH_2Cl_2 and chromatographed (same conditions as for **14**): [$Ir_2Rh_2(CO)_8$ (η^4-cod)$_2$] (346 mg, 54%). Red crystals. IR (CH_2Cl_2): 2054*vs*, 2032*s*, 1997*s*, 1960*m*, 1860*w*, 1817*s* (CO). ^{13}C-NMR (CD_2Cl_2, 200 K): 249.8 (*t*, J(C,Rh) = 31, *a*); 228.2 (*d*, J(C,Rh) = 30, *b*); 174.0, 166.6, 166.1, 160.1 (4*s*, *d*, *e*, *g*, *c*); rel intensities 1:2:1:1:2:1. 2D-COSY: cross-peak between *e* and *c*. Simulation of VT-^{13}C-NMR (T[K], k[s^{-1}]): 255, 17; 260, 29; 265, 55; 270, 86; 275, 113; 280, 165; 290, 380; 300, 871. Anal. calc. for $C_{24}H_{24}Ir_2O_8Rh_2$ (1030.7): C 27.97, H 2.35, Ir + Rh 57.27; found: C 27.95, H 2.30, Ir + Rh 57.12.

REFERENCES

[1] S. Martinengo, P. Chini, V.G. Albano, F. Cariati, T. Salvatori, *J. Organomet. Chem.* **1973,** *59,* 379.

[2] B.F.G. Johnson, J. Lewis, T.W. Matheson, *J. Chem. Soc., Chem. Commun.* **1974,** 441; J. Evans, B.F.G. Johnson, J. Lewis, T.W. Matheson, J.R. Norton, *J. Chem. Soc., Dalton Trans.* **1978,** 626; I.T. Horváth, *Organometallics* **1986,** *56,* 2333.

[3] V.G. Albano, G. Ciani, S. Martinengo, *J. Organomet. Chem.* **1974,** *78,* 265.

[4] G. Bondietti, G. Suardi, R. Ros, R. Roulet, F. Grepioni, D. Braga, *Helv. Chim. Acta* **1993,** *76,* 2913.

[5] T.A. Pakkanen, J. Pursiainen, T. Venäläринen, T.T. Pakkanen, *J. Organomet. Chem.* **1989,** *372,* 129.

[6] G. Bondietti, R. Ros, R. Roulet, F. Grepioni, D. Braga, *J. Organomet. Chem.* **1994,** *464,* C45.

[7] J. Evans, B.F.G. Johnson, J. Lewis, J.R. Norton, *J. Chem. Soc., Chem. Commun.* **1973,** 807.

[8] A. Strawczynski, R. Ros, R. Roulet, *Helv. Chim. Acta* **1988,** *71,* 867.

[9] B.E. Mann, C.M. Spencer, A.K. Smith, *J. Organomet. Chem.* **1983,** *244,* C17; B.E. Mann, B.T. Pickup, A.K. Smith, *J. Chem. Soc., Dalton, Trans.* **1989,** 889.

[10] A. Strawczynski, G. Suardi, R. Ros, R. Roulet, *Helv. Chim. Acta* **1993,** *76,* 2210.

[11] G. Laurenczy, G. Bondietti, A.E. Merbach, B. Moullet, R. Roulet, *Helv. Chim. Acta* **1994,** *77,* 547.

[12] A. Strawczynski, R. Ros, R. Roulet, F. Grepioni, D. Braga, *Helv. Chim. Acta* **1988,** *71,* 1885.

[13] R.J. Crowte, J. Evans, M. Webster, *J. Chem. Soc., Chem. Commun.* **1984,** 1344.

[14] G. Suardi, A. Strawczynski, R. Ros, R. Roulet, F. Grepioni, D. Braga, *Helv. Chim. Acta* **1990,** *73,* 154; A. Orlandi, U. Frey, G. Suardi, A.E. Merbach, R. Roulet, *Inorg. Chem.* **1992,** *31,* 1304.

[15] A. Strawczynski, C. Hall, G. Bondietti, R. Ros, R. Roulet, *Helv. Chim. Acta* **1994,** *77,* 754.

[16] G.F. Stuntz, J.R. Shapley, *J. Organomet. Chem.* **1981,** *213,* 389.

[17] A. Orlandi, R. Ros, R. Roulet, *Helv. Chim. Acta* **1991,** *74,* 1464.

[18] K. Besançon, G. Laurenczy, T. Lumini, R. Roulet, G. Gervasio, *Helv. Chim. Acta* **1993,** *76,* 2926.

---

[3]) Labelling as follows: bridged CO's, *a*, and *b*, with *a* linked to the two basal Rh-atoms; radial CO, *d* (bonded to Ir); axial CO, *c* (bonded to Ir); apical CO's, *e* and *g*.